Reinforcement Effects of Microfibrillated Cellulose on Chitosan–Polyvinyl Alcohol Nanocomposite Film Properties

Achmad Solikhin Yusuf Sudo Hadi Muh Yusram Massijaya
Siti Nikmatin Shigehiko Suzuki Yoichi Kojima Hikaru Kobori

Abstract

The objective of this research was to analyze the reinforcement effect of microfibrillated cellulose (MFC) on chitosan–polyvinyl alcohol (chitosan-PVA) nanocomposite films in terms of their morphological, physical, chemical, thermal, biological, and mechanical properties. Chitosan-PVA blend films reinforced with MFC filler loadings at 0.5 to 5 percent had smoother, more regular, and more uniform external surface morphology compared with chitosan-PVA reinforced with MFC filler loaded at 7.5 percent. With regard to the physical properties, incorporation of MFC into chitosan-PVA polymer blends reduced nanocomposite film transparency. Furthermore, the films had three different diffraction peaks: crystalline peak, amorphous peak, and small ancillary peak. Compared with the neat chitosan-PVA blend, the addition of MFC to chitosan-PVA polymer blends shifted Fourier-transform infrared spectroscopy peaks at 3,500 to 3,000, 2,918, 1,440, 1,101, and 850 cm^{-1}, indicating a chemical interaction between chitosan-PVA polymer blends and MFC. According to differential scanning calorimetry, thermogravimetric analysis, and differential thermal analysis, the addition of MFC enhanced the thermal stability of chitosan-PVA compared with neat chitosan-PVA composite films. Most nanocomposite films reinforced with MFC had a higher tensile strength than films made from neat chitosan-PVA and chitosan-PVA-MFC 7.5 percent because of percolation formation. However, neither neat chitosan-PVA composite film nor chitosan-PVA-MFC nanocomposite films showed a zone of inhibition or had a zone of inhibition index against *Escherichia coli*, *Staphylococcus aureus*, *Candida albicans*, and *Ganoderma* sp.

Most composite films derived from petroleum-based polymers have recently come under scrutiny by scientists in the food and packaging industry worldwide due to the negative impact of these films on health and ecology. Minimizing the negative impact of petroleum-based materials is also important in lessening our dependency on fossil fuels. Blending a synthetic polymer with a biopolymer is one solution to overcoming the problems associated with petroleum-based composite films. As an example, combining chitosan with polyvinyl alcohol (PVA) creates a biosynthetic polymer blend that has shown promise in several studies (Nakano et al. 2007, El-Hefian et al. 2010, Casey and Wilson 2015, Abraham et al. 2016).

Aside from addressing ecological concerns, a blend of these polymers may minimize the drawbacks of each single polymer, widen the applications of the resultant films, and create new composite films that have improved properties. Chitosan biopolymer alone has inferior properties, including low flexibility, brittleness, and fragility (Pavaloiu et al. 2014). It also has poor chemical stability, low mechanical strength, and a complicated recovery process (Zhou et al. 2014). PVA polymer alone is costly and synthetic, and it biodegrades slowly (Panaitescu et al. 2015). It also provides a poor moisture barrier (Azizi et al. 2014a). The mechanical strength of composite films manufactured from

The authors are, respectively, Doctoral Student, Professor, and Professor, Biocomposite Lab., Faculty of Forestry, Bogor Agric. Univ., Bogor, Indonesia (achmad_solikhin@apps.ipb.ac.id, yshadi@indo.net.id [corresponding author], mymassijaya@yahoo.co.id); Associate Professor, Dept. of Physics, Faculty of Mathematics and Natural Sci., Bogor Agric. Univ., Bogor, Indonesia (snikmatin@apps.ipb.ac.id); and Professor, Associate Professor, and Associate Professor, Dept. of Environ. and Forest Resources Sci., Faculty of Agric., Shizuoka Univ., Shizuoka, Japan (suzuki.shigehiko@shizuoka.ac.jp, kojima.yoichi@shizuoka.ac.jp, kobori.hikaru@shizuoka.ac.jp). This paper was received for publication in April 2017. Article no. 17-00028.

Forest Prod. J. 68(3):216–225.
doi:10.13073/FPJ-D-17-00028

a blend of chitosan and PVA was found to be increased (Abraham et al. 2016), and its swelling degree was also higher (El-Hefian et al. 2010). For use as a film in food packaging, the water vapor and oxygen barriers of a blend must be excellent.

To improve the properties of the polymer blend for composite films, nanosized organic agents have been utilized for reinforcement because of their excellent mechanical properties, oxygen gas barrier properties, low toxicity, renewability, biodegradability, and low density (Solikhin et al. 2017a). Prior studies have investigated various reinforcement agents, including nanocrystalline cellulose (Kermani and Esfandiary 2016), cellulose nanocrystals (Azizi et al. 2014b), multiwalled carbon nanotubes (Abdolrahimi et al. 2016), gelatin nanoparticles (Fathollahipour et al. 2015), and cellulose nanofibers (Choo et al. 2016). However, incorporation of nanofillers can reduce the tensile strength, tensile modulus, thermal stability, and water and oxygen barrier properties of composite films. Additives have also been incorporated into chitosan-PVA composite films to provide novel features, such as cloisite 30B (Parida et al. 2011) for controlled release of curcumin as an anticancer drug, nitrofurazone (Kouchak et al. 2014) and ZnO-Ag (Azizi et al. 2014a) for antibacterial effects, and aqueous mint extract/pomegranate peel extract (Kanatt et al. 2012) for antioxidant activities.

Another reinforcing agent is microfibrillated cellulose (MFC), which is often referred to as nanofibrillated cellulose. The diameter of individual MFC fibers is on the nanometric scale ($<$100 nm), and MFC has the potential to be a reinforcing agent because of its large and active surface area. MFC has previously been utilized to enhance the properties of chitosan (Liu et al. 2013) and PVA (Lu et al. 2008) composite films, and benefits included good mechanical properties, good chemical resistance, and material biodegradability. However, the use of MFC to reinforce chitosan-PVA nanocomposite films has not yet been studied.

The objective of this study was to analyze the morphological, physical, chemical, thermal, biological, and mechanical properties of chitosan-PVA nanocomposite films containing MFC. Furthermore, the morphological, physical, chemical, thermal, antibacterial and antifungal, and mechanical properties were determined by scanning electron microscope, X-ray diffraction, Fourier-transform infrared (FTIR) spectroscopy differential scanning spectroscopy and thermogravimetry analyzer, agar diffusion test, and universal testing machine, respectively.

Materials and Methods

Materials

Air-dried oil palm empty fruit bunch (OPEFB; PT Perkebunan Nusantara VIII, Bogor, Indonesia) fibers were used to isolate MFC by means of steam explosion, which was assisted with ultrasonication. Other materials used were chitosan (Biotech Surindo, Cirebon, Indonesia) with the following specifications: an acetylation degree of 85.13 percent (w/w), white appearance, viscosity of 355.5 cps, moisture content of 10.68 percent, ash content of 1.29 percent, particle size of 20 to 30 mesh, and fully hydrolyzed PVA (Merck KGaA, Darmstadt, Germany). Analytical-grade chemicals included 98 percent acetic acid, 30 percent hydrogen peroxide, 98 percent formic acid, and sodium hydroxide (Merck). *Escherichia coli* and *Staphylococcus aureus* (IPB Culture Collection, Bogor, Indonesia); a dimorphic fungus, *Ganoderma* sp. (Forest Pathology Laboratory, Silviculture Department, IPB, Bogor, Indonesia); and *Candida albicans* were used to test antibacterial and antifungal properties of the nanocomposite films.

Isolation of OPEFB microfibrillated cellulose

MFC isolation was undertaken according to Solikhin et al. (2017a) by means of steam explosion assisted with ultrasonication. OPEFB vascular bundles were pulverized with dry disk milling for 27 minutes and sieved with a 100-mesh sieve analyzer. Two grams of microparticles were added to a mixture of 5 percent sodium hydroxide and 5 percent hydrogen peroxide and then autoclaved under a pressure of 1.5 bar at 121°C for 1 hour. Autoclaved microparticles were washed several times with deionized water and then added to a mixture of 10 percent hydrogen peroxide and 20 percent formic acid solution (ratio of 1:1). The particles were heated in a shaking bath at 85°C and 75 rpm for 2 hours and subsequently washed with deionized water. The particles were suspended in a mixture of 5 percent hydrogen peroxide and 5 percent sodium hydroxide and heated in a shaking water bath at 60°C and 90 rpm for 90 minutes. The mixture was steam-exploded by using an autoclave at 121°C and 1.5 bar for 1 hour and washed with deionized water several times. Obtained cellulose was further homogenized in an Ultraturax homogenizer (Janke & Kunkel GmbH & Co. KG, Staufen, Germany) at a rate level of 7 for 20 minutes (220 V, 600 W, and 24,000/cm). To isolate MFC, fibrillated cellulose (1 g) was subsequently suspended in deionized water (200 mL) and ultrasonicated (Ultrasonic Processor; Cole Parmer Instrument, Vernon Hills, Illinois, USA). The ultrasonication process was undertaken in an ice-water bath for 25 minutes with the following parameters: an amplitude of 40 percent, power of 130 W, and frequency of 20 kHz.

Fabrication of chitosan-PVA with microfibrillated cellulose

Chitosan powder (1 wt%) was dissolved in 1 percent CH_3COOH and subsequently stirred at a rate of 100 rpm for 4 hours. Fully hydrolyzed PVA (5 wt%) was dissolved in deionized water at 90°C and mechanically stirred at 100 rpm for 4 hours to produce a PVA solution. Chitosan-PVA nanocomposite films were fabricated by mixing chitosan and PVA solution at a ratio of 1:1 (40 mL:40 mL). Next, 10 mL of MFC solution was added to solutions with varying concentrations of chitosan and PVA (0, 0.5, 1, 1.5, 2.5, 5, and 7.5% total weight). The mixtures were mechanically stirred at 35°C and 1,200 rpm for 19 hours for good dispersion, and they were then solvent-casted in a polypropylene plate for 3 days to evaporate water. The casted mixtures were then degassed in a desiccator to ensure the production of high-quality films, and the films were subsequently oven-dried at 45°C for 24 hours. The chitosan-PVA nanocomposite films obtained were denoted as neat chitosan-PVA, chitosan-PVA 0.5 percent, chitosan-PVA-MFC 1 percent, chitosan-PVA-MFC 1.5 percent, chitosan-PVA-MFC 2.5 percent, chitosan-PVA-MFC 5 percent, and chitosan-PVA-MFC 7.5 percent.

Characterization

An ultraviolet-visible spectrophotometer (USB4000 Miniature Fiber Optic Spectrometer; Ocean Optics Inc., Dunedin, Florida, USA) was used to investigate the transparency of the nanocomposite films, with the analysis being conducted at wavelengths between 200 and 850 nm. A scanning electron microscope (JSM-6510; JEOL Ltd, Tokyo, Japan) was utilized to analyze the external and fracture morphology of the films, and the analysis was carried out at 15 kV. Prior to the analysis, the films were ultra-thin-coated with platinum to inhibit charging during scanning electron microscopic analysis. A diffraction profile of the films was investigated by means of an X-ray diffraction (XRD 6100; Shimadzu, Kyoto, Japan). A Cu Kα irradiation with 40 kV/30 mA, $\lambda = 1.54$ Å, and XRD degree at $2\theta = 5°$ to 45°, with a step of $2\theta = 0.02°$, was used for the analysis. FTIR (FT-IR 8400 S; Shimadzu, Tokyo, Japan) was utilized to analyze functional group changes of the films, and scans were carried out in a wavenumber range of 700 to 4,000 cm^{-1} with a resolution of 2 cm^{-1}. Thermal stabilities of the films were analyzed with differential scanning calorimetry (DSC-60; Shimadzu), a thermogravimetry analyzer (Rigaku, Tokyo, Japan), and a differential thermogravimetry analyzer (Rigaku). Differential scanning calorimetry was performed at a nitrogen atmosphere gas flow of 20 mL/min in a temperature range of 0°C to 400°C at a rate of 10°C/min. A thermogravimetry analyzer combined with a differential thermal analyzer was operated under air atmosphere gas flux at a rate of 4°C/min in the temperature range of 0°C to 400°C. The tensile strength of the films was assessed by means of a UTM (AGS-X Series; Shimadzu) at a crosshead speed of 5 mm/min using a 1-kN static load cell and a gauge length of 50 mm. The tested films were each 10 cm in length and 2.54 cm in width.

For antibacterial properties, zone of inhibition (ZOI) sizes and ZOI indices (ZOIIs) were used as response variables to test how well the films protected against *E. coli* and *S. aureus*. An agar diffusion test was performed, using bacteria culture media at a concentration of 10^7 CFU/mL made from trypticase soy agar (40 g) in 1 liter of distilled water. Film samples (diameter 5 mm) were incubated in petri dishes for 48 hours at 37°C. To test the fungicidal and fungal inhibition properties of the composites, *C. albicans* and *Ganoderma* sp. were used in tests based on the agar diffusion method. Prior to the tests, potato dextrose agar was prepared (about 40 g) in 1 liter of distilled water for the culture media. The incubation was carried out for 2 days for *C. albicans* (10^6 CFU/mL) and 19 days for *Ganoderma* sp. (10^5 CFU/mL) at room temperature.

Results and Discussion

Ultraviolet visible spectrophotometry

Chitosan-PVA nanocomposite films reinforced with different MFC concentrations and having thicknesses of 0.10 to 0.18 μm had variable optical properties. The increase in MFC concentration was associated with a decrease in the transmittances of the films in a wavelength range of 400 to 800 nm. The decrease in transmittances implicitly indicated that the transparency of the films was diminished by MFC self-agglomeration becoming a barrier to light penetration (Ching et al. 2015). The agglomeration is irreversible during solvent casting, but reversible agglomeration can be achieved by solvent exchanges, chemical surface modification, and surfactant uses.

The transmittances of films at wavelengths of 400, 500, 600, and 700 nm are presented in Table 1. Neat chitosan-PVA film had better optical properties: 99.43, 96.46, 96.52, and 96.69 percent. With individual MFC fibers with a diameter of approximately 100 nm, light would be easily scattered in the chitosan-PVA blend, inducing a high transmittance percentage. In contrast, with aggregated MFC fibers with diameters above 100 nm, light scattering would be impeded, resulting in low transmittance percentages (reduced visibility).

Scanning electron microscope

Figure 1 presents scanning electron micrographs of the external surfaces of the films made with chitosan-PVA reinforced with MFC. Neat chitosan-PVA films had very smooth and regular external surfaces compared to those made with chitosan-PVA reinforced with MFC. The addition of filler loading at 0.5 to 5 percent into the chitosan-PVA blends produced slightly smoother, regular, and uniform external surfaces of chitosan-PVA composite films. This finding was similar to outcomes in previous research (Choo et al. 2016, Shankar and Rhim 2016). These properties seem to be explained by the percolation theory by which a rigid hydrogen-bonded network of MFC forms (Zhou et al. 2012), resulting in good compatibility between the chitosan-PVA blends and MFC.

An MFC filler loading at 7.5 percent led to aggregated fibers (spots) on the surface of chitosan-PVA nanocomposite films (Fig. 1f). Some white-colored spots were observed in these films, likely due to the magnitude of hydrogen bonding and van der Waals forces of the MFC fibers, which were pulled to the external surface of the film. The presence of these spots may cause a stress concentration that could adversely influence the mechanical properties of the films, a point that will be discussed later.

X-ray diffraction

Figure 2 shows the diffraction pattern of chitosan-PVA nanocomposite films reinforced with MFC. Most of the diffraction patterns were slightly changed in the crystalline, amorphous, and small ancillary peak regions. Three diffraction peaks were observed: a crystalline peak at $2\theta = 11.42°$ to 11.91°, an amorphous peak at $2\theta = 19.66°$ to 19.83°, and a small ancillary peak at $2\theta = 40.62°$ to 41.03°. Choo et al. (2016) stated that PVA/chitosan films had three indispensable peaks, which were at $2\theta = 11.3°$ (crystalline

Table 1.—Optical properties of chitosan–polyvinyl alcohol (PVA) reinforced with microfibrillated cellulose (MFC) at 400, 500, 600, and 700 nm.

Sample name	Transmittance (%)			
	400 nm	500 nm	600 nm	700 nm
Chitosan-PVA	99.4	96.5	96.5	96.7
Chitosan-PVA-MFC 0.5%	85.7	87.1	87.8	88.1
Chitosan-PVA-MFC 1%	82.4	83.9	85.3	86.2
Chitosan-PVA-MFC 1.5%	79.7	81.9	83.4	84.5
Chitosan-PVA-MFC 2.5%	70.9	74.1	75.6	76.4
Chitosan-PVA-MFC 5%	65.6	66.1	68.0	69.3
Chitosan-PVA-MFC 7.5%	44.7	45.7	46.2	46.9

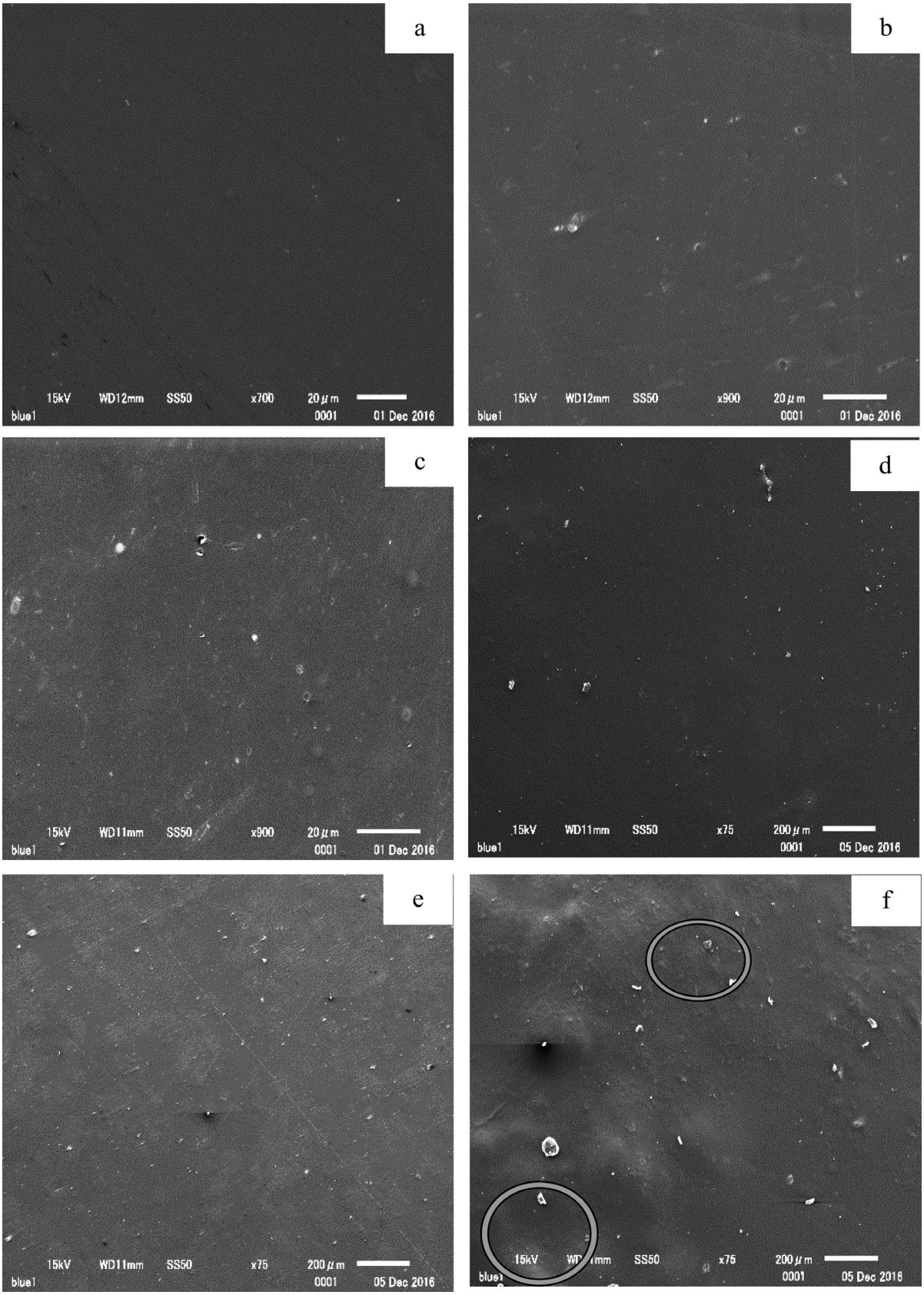

Figure 1.—Scanning electron micrographs of chitosan–polyvinyl alcohol film reinforced with microfibrillated cellulose: (a) neat, (b) 0.5 percent, (c) 1.5 percent, (d) 2.5 percent, (e) 5 percent, and (f) 7.5 percent.

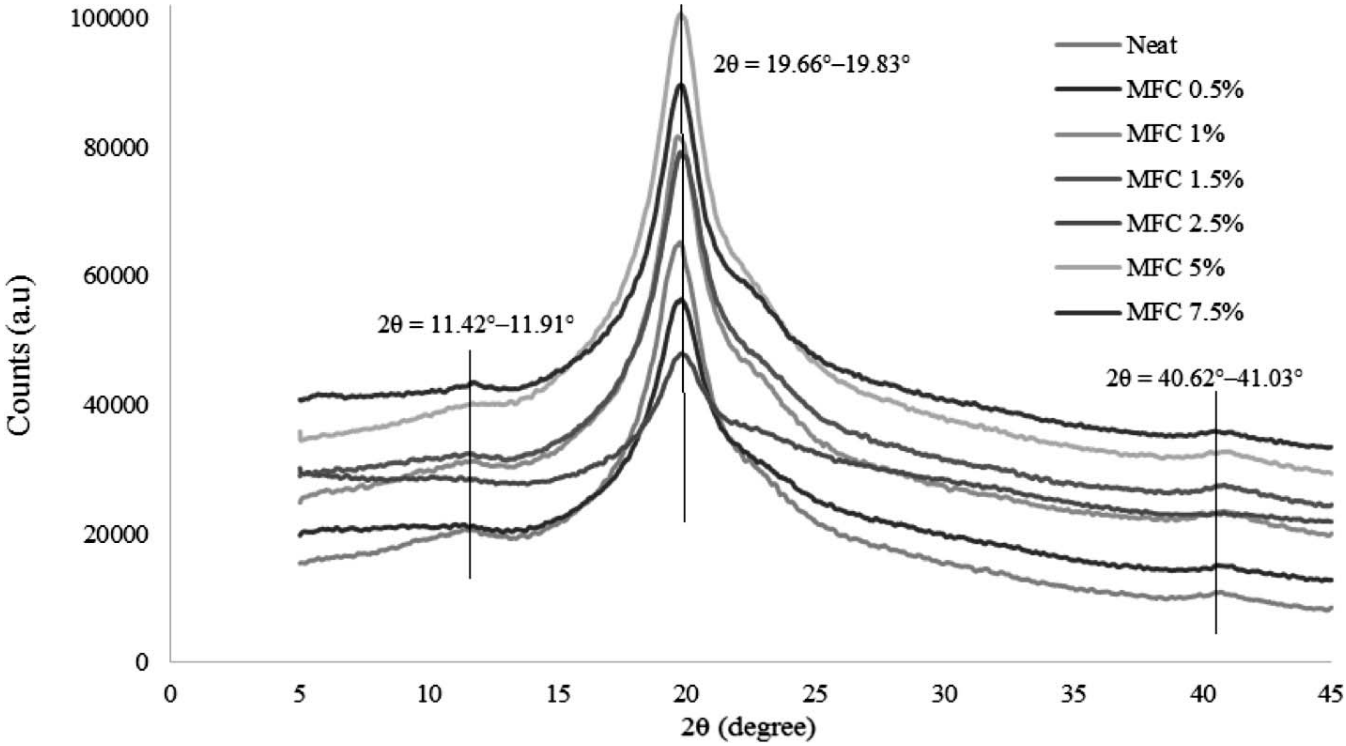

Figure 2.—X-ray diffraction pattern of chitosan–polyvinyl alcohol composite films reinforced with different microfibrillated cellulose (MFC) concentration.

state), $2\theta = 19.4°$ (amorphous state), and $2\theta = 22.8°$ (lower intensity of chitosan diffractogram peak).

Neat chitosan-PVA composite films had a crystalline peak at 11.56°, an amorphous peak at 19.74°, and a shoulder peak at 40.47°. Several shifts of these peaks occurred with the addition of MFC. The reinforcement of chitosan-PVA with MFC slightly increased 2θ diffractograms for the amorphous and shoulder peaks, whereas the diffractograms for the crystalline peaks varied slightly. The reinforcement with MFC appeared to enhance the molecular ordering of amorphous state of the films by slightly altering the structural uniformity (crystallinity peak) of chitosan-PVA polymer blends (Azizi et al. 2014b, Choo et al. 2016). The slight alteration of the peak or state was presumably due to a small concentration of MFC incorporated into the composite (Shankar and Rhim 2016).

The increase in 2θ diffractograms and intensities of tested chitosan-PVA-MFC nanocomposite films was also presumably due to the crystallinity effects and indices of the MFC. According to Solikhin et al. (2017a), MFC materials exhibit a higher crystallinity than raw OPEFB microfibers (Solikhin et al. 2016) and lignocellulose nanofibers (Solikhin et al. 2017b). The MFC crystallites function as a nucleating agent, contributing to the crystallites of the polymer blends of chitosan-PVA bundling together.

FTIR spectroscopy

Chemical functional groups shifted in response to MFC being added to the chitosan-PVA polymer blends (Fig. 3; Table 2). A notable change occurred in the FTIR spectra when the chitosan-PVA nanocomposite films were reinforced by MFC. The transmittance band in the range of 3,000 to 3,500 cm^{-1} indicated the presence of a hydroxyl group stretching vibration for MFC and PVA and the presence of an amide functional group of chitosan. A peak of 2,918 cm^{-1} was assigned to the presence of a CH_2 stretching vibration (El-Hefian et al. 2010, Parida et al. 2011), which indicated the presence of hydrogen bonds among PVA, chitosan, and MFC.

Transmittance intensities at the peaks of 1,712, 1,654, and 1,568 cm^{-1} were shifted along with the higher MFC filler loading, attributable to the presence of C=O, C-O, and $-NH_3^+$ functional groups, respectively. The presence of C=O and C-O was influenced by the residual acetic acid used for dissolving chitosan polymer (Pouranvari et al. 2016) or by the remaining acetate groups in PVA during the saponification reaction of polyvinyl acetate (PVAc) (Alhosseini et al. 2012). The NH_3^+ represented the ionization process of chitosan amino groups in the acidic media (Pouranvari et al. 2016).

Other important peaks at 1,440, 1,101, and 850 cm^{-1} were ascribed to CH-O-H vibration, C-O stretching vibration, and C-C stretching (Parida et al. 2011, Alhosseini et al. 2012, Santos et al. 2014), respectively. Another broad peak at a transmittance peak of 615 cm^{-1} was indicated with the crystallization of chitosan (Chen et al. 2007). However, the incorporation of MFC into chitosan-PVA blends lowered the FTIR spectra due to a strong intermolecular and intramolecular hydrogen bond between the PVA-chitosan polymer blend and MFC.

Differential scanning calorimetry

The glass transition (Tg), melting point (Tm), maximum degradation temperature, and enthalpy of chitosan-PVA composite films reinforced with MFC are shown in Table 3. Figure 4 illustrates the four steps of thermal degradation of

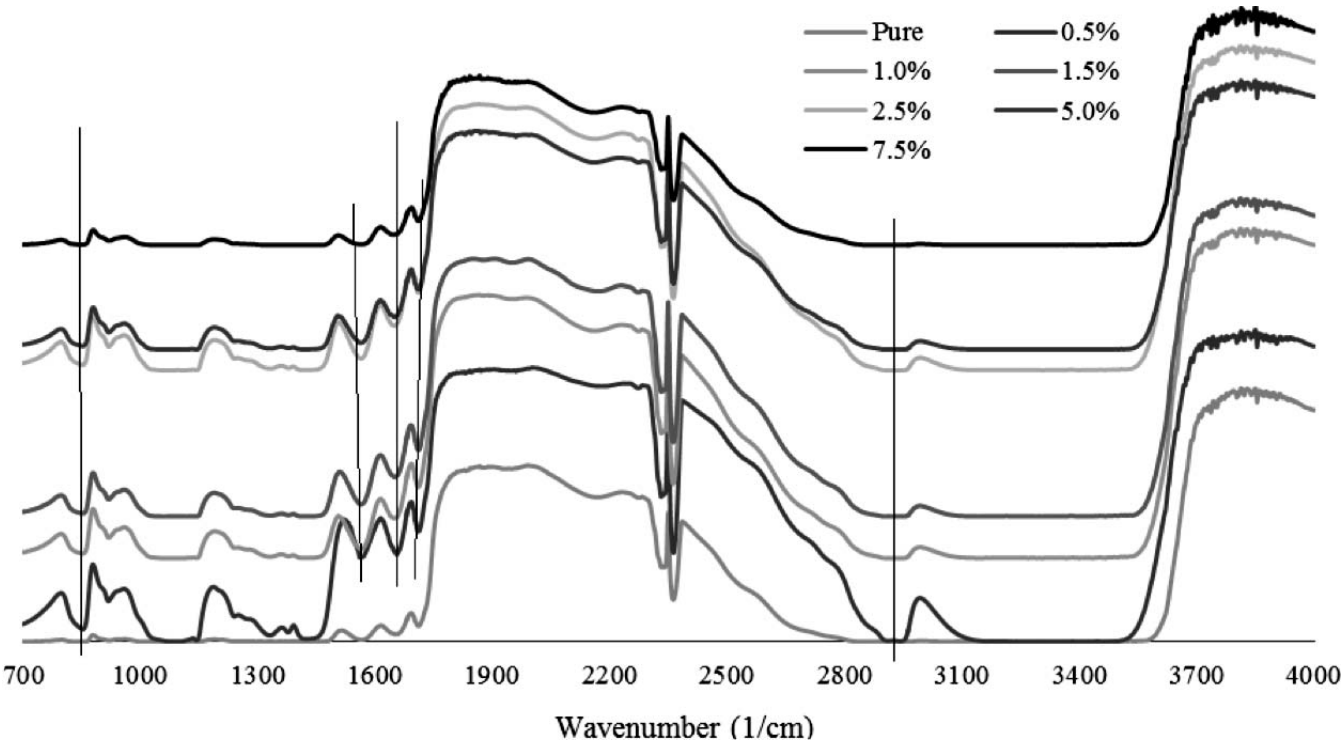

Figure 3.—Fourier-transform infrared spectra of chitosan–polyvinyl alcohol–microfibrillated cellulose composite films.

the nanocomposite films, including (1) the glass transition, (2) melting point, and (3) two maximum thermal degradation peaks. The addition of MFC notably increased the glass transition temperature of the chitosan-PVA nanocomposite films from 60.7°C to 67.4°C, but it decreased the melting point temperature (124.4°C to 145.6°C) of the films. The increase and decrease in Tg and Tm were presumably due to the influence of hydroxyl groups and crystallinity, respectively.

Besides the abundance of hydroxyl groups of PVA and chitosan, MFC possessed a higher number of hydroxyl groups, which contributed to the strong hydrogen bonding between chitosan-PVA polymer blend and MFC and thereby restricted the segmental mobility of the polymer chains (Zhou et al. 2012, Santos et al. 2014). The decrease in Tm was due to the partial miscibility between chitosan-PVA polymer blends with MFC (Chen et al. 2007), resulting in agglomeration. The agglomeration of MFC further induced a steric hindrance effect, restricting the growth of crystalline PVA and semicrystalline chitosan regions (Zhou et al. 2012). Most of the first and second maximum degradation temperature peaks increased, which was in concordance with the addition of MFC and indicated the formation of strong hydrogen bonding between the polymer blends and nanofillers.

Thermogravimetry/differential thermal analyzer

Figure 5 shows the thermogravimetry/differential thermal analysis of the thermal stability of chitosan-PVA nanocomposite films reinforced with MFC. The films had three transition phases of thermal degradation, consisting of water evaporation, structural degradation, and carbonaceous matter degradation (Fig. 5a). In all tested neat and chitosan-PVA-MFC composite films, weak physically free and bound water in the films began to evaporate (35% water

Table 2.—Fourier-transform infrared analysis of neat chitosan–polyvinyl alcohol (PVA) and chitosan–PVA–microfibrillated cellulose composite films.

Wavelength (1/cm)	Chemical functional groups	Chitosan-PVA composite films						
			Microfibrillated cellulose					
		Neat	0.5%	1%	1.5%	2.5%	5%	7.5%
3,500–3,000	-OH stretching vibration and O=C-N	—	√	√	√	√	√	√
2,918	CH_2 stretching vibration	—	√	√	√	√	√	√
1,712	C=O	√	√	√	√	√	√	√
1,654	C-O	√	√	√	√	√	√	√
1,568	$-NH_3^+$	√	√	√	√	√	√	√
1,440	CH-O-H vibration	—	√	√	√	√	√	√
1,101	C-O stretching vibration	—	√	√	√	√	√	√
850	C-C stretching	—	√	√	√	√	√	√

Table 3.—Thermal properties of chitosan–polyvinyl alcohol (PVA) composite films.[a]

Sample	Tg (°C)	Tm (°C)	ΔHf (J/g)	Tmax 1 (°C)	ΔHf (J/g)	Tmax 2 (°C)	ΔHf (J/g)
Chitosan-PVA	60.7	145.6	−11.1	214.3	−33.6	298.6	−271.5
Chitosan-PVA-MFC 0.5%	63.5	131.3	−54.1	214.7	−51.4	308.0	−204.8
Chitosan-PVA-MFC 1%	63.5	135.5	−49.5	213.6	−46.1	305.9	−209.0
Chitosan-PVA-MFC 1.5%	65.4	127.5	−48.9	215.9	−54.0	311.9	−261.4
Chitosan-PVA-MFC 2.5%	65.0	121.5	−57.6	215.9	−58.8	310.2	−230.2
Chitosan-PVA-MFC 5%	67.4	124.4	−40.0	215.5	−47.4	305.6	−234.4
Chitosan-PVA-MFC 7.5%	67.0	113.1	−42.8	217.6	−30.9	292.1	−241.7

[a] Tg = glass transition; Tm = melting point; Hf = heat fusion; Tmax = maximum degradation temperature; MFC = microfibrillated cellulose.

weight loss) at temperatures ranging from 40°C to 190°C. The addition of MFC (1% to 5%) to the chitosan-PVA polymer blends induced slow weight loss due to evaporation in this temperature range, while the chitosan-PVA-MFC 0.5 percent film had an increase in weight loss due to free and bound water effects. The presence of water in the films acted as a plasticizing agent that improved the movement of chitosan-PVA polymer blends, decreased the polymer crystallinity, and prevented intra- and intermolecular hydrogen bonding between chitosan-PVA and MFC. At the second stage (210°C to 350°C), the reinforcement with MFC notably increased major degradation temperature. The stage was attributable to the structural degradation of chitosan-PVA, dehydration, and pyrolysis of MFC, generating volatile products (Frone et al. 2011). The differential thermal analysis shown in Figure 5b confirmed that the chitosan-PVA blends reinforced with MFC had enhanced thermal stability due to strong hydrogen bonding between MFC and chitosan-PVA polymer blends (Zhou et al. 2012). The third degradation zone was attributable to the carbonaceous matter degradation (over 350°C), and its temperature was enhanced by the addition of MFC, as indicated by the appearance of a small exothermic peak around 350°C to 380°C (Fig. 5b). In summary, the addition of MFC enhanced the thermal stability of chitosan-PVA over neat chitosan-PVA composite films.

Tensile strength

Figure 6 demonstrates the tensile strength of the neat and chitosan-PVA-MFC nanocomposite films. Most of the tested composite films reinforced with MFC exhibited a higher tensile strength than the neat chitosan-PVA films. The optimum tensile strength occurred in the chitosan-PVA composite films with an MFC filler loading of 5 percent (77.44 N/mm^2). These films had an increase in tensile strength that was 57 percent higher than that of the neat chitosan-PVA films. The decrease in tensile strength of chitosan-PVA-MFC 7.5 percent was presumably due to self-aggregation and nonhomogeneous distribution of MFC, creating stress concentrations. The higher tensile strength with MFC reinforcement was expected due to the formation of a percolation network structure that resulted from the

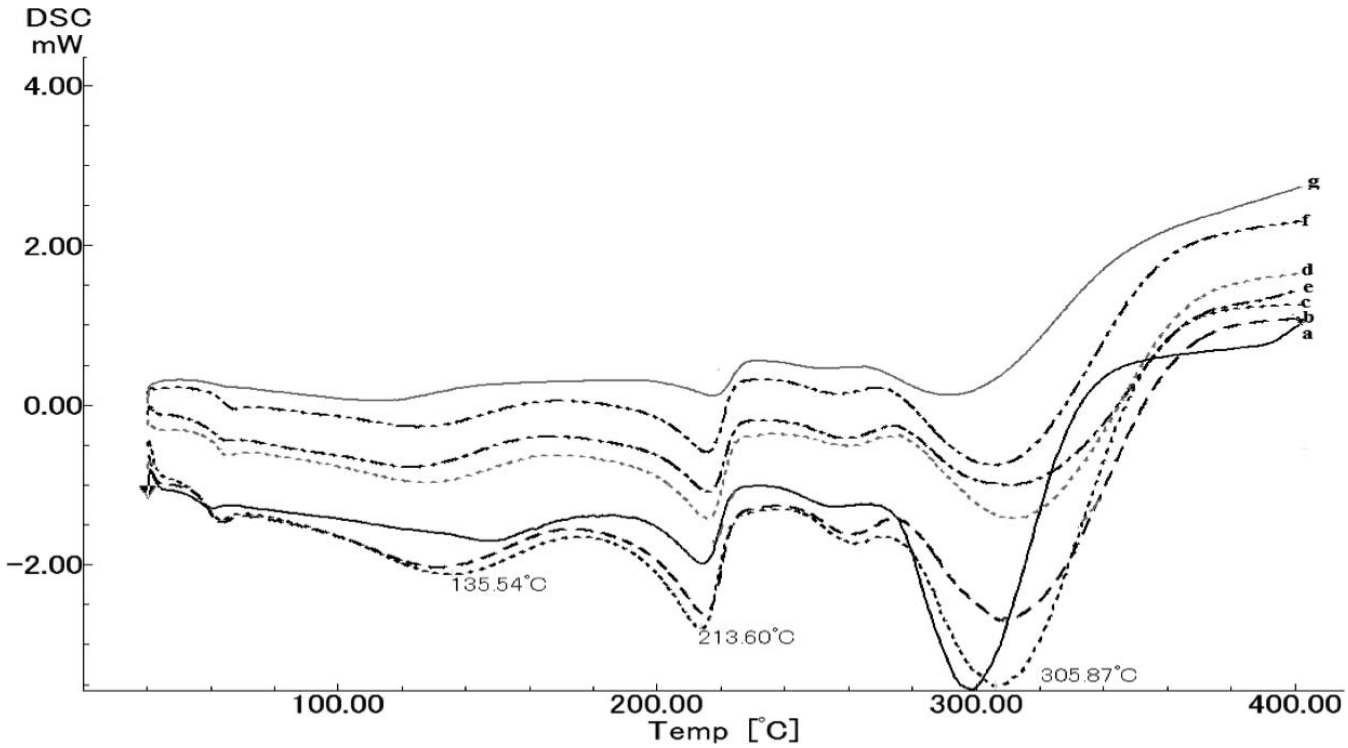

Figure 4.—Thermal stability analysis of chitosan–polyvinyl alcohol polymer blend reinforced with microfibrillated cellulose: (a) neat, (b) 0.5 percent, (c) 1 percent, (d) 1.5 percent, (e) 2.5 percent, (f) 5 percent, and (g) 7.5 percent.

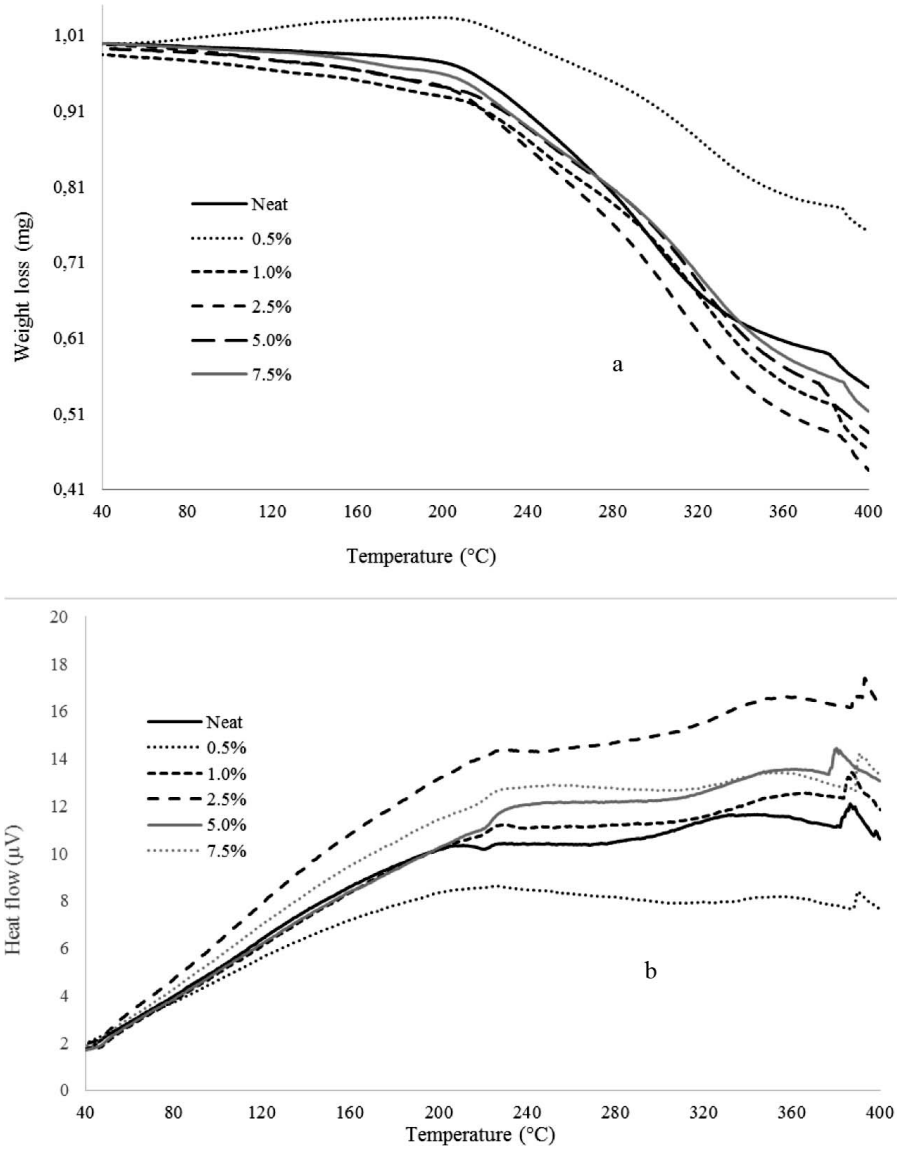

Figure 5.—Thermogravimetric analysis (a) and differential thermal analysis (b) thermal properties of chitosan–polyvinyl alcohol nanocomposite films.

filler–matrix interactions in the composites. This network structure likely increased hard portion crystallinity, decreased molecular mobility, and promoted rigidity (Azizi et al. 2014a).

Polynomial regression showed that the tensile strength values were normally distributed with a formula of $y = -2.7814x^2 + 18.864x + 49.764$ and $R^2 = 0.6924$ and an optimum reinforcing agent concentration of 3.39 percent. The formula indicated that the polynomial regression fitted the distribution value of chitosan-PVA-MFC nanocomposite films' tensile strength. The R^2 obtained from the quadratic (polynomial) regression could have been affected by other factors that were not accounted for, such as the dimension of the samples, weight of the samples, and crystallinity size and index. A better percolation network is in accordance with Figure 1, which shows good dispersion and compatibility of chitosan-PVA composite films at MFC concentrations of 0.5 to 5 percent, whereas an MFC concentration of 7.5 percent was associated with aggregation. This aggregation led to discontinuity in the films that affected its mechanical properties.

Antibacterial and antifungal properties

Table 4 summarizes the antibacterial and antifungal properties of chitosan-PVA-MFC nanocomposite films against *E. coli*, *S. aureus*, *C. albicans*, and *Ganoderma* sp. In this test, only four samples were tested, including neat chitosan-PVA and chitosan-PVA reinforced with MFC 2.5 percent, MFC 5 percent, and MFC 7.5 percent. Neat chitosan-PVA composite films did not show a ZOI or a ZOII against these bacteria and fungi. Similar results were obtained for chitosan-PVA blends reinforced with MFC. Although the chitosan was expected to provide antimicrobial activity and efficacy, it did not appear to act as a bactericidal or fungicidal agent. These results are similar to those of prior studies (Arora et al. 2011, Ostadhossein et al. 2015).

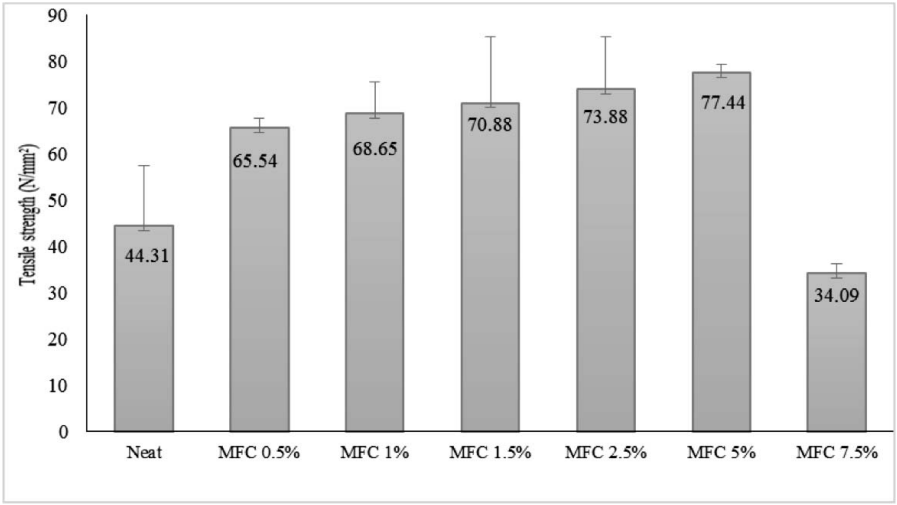

Figure 6.—Chitosan–polyvinyl alcohol composite films' tensile strength. MFC = microfibrillated cellulose.

We speculate that the lack of antibacterial and antifungal properties was due to the intermolecular and intramolecular hydrogen bonds between the amine groups of chitosan and the hydroxyl groups of PVA and MFC. Such bonds could have prevented interaction between the cationic chitosan structure and the negatively charged moieties of the bacterial and fungal cell membranes. Consequently, there was no disturbance of the membranes that would have otherwise led to rupture and cell death. In addition, a lower degree of deacetylation generated lower positive charges of chitosan-PVA blends, further reducing any impact that interaction with the cell walls would have had. Other factors that could affect the antibacterial and antifungal properties of the films included chitosan viscosity, bacteria type (gram positive or gram negative), hydrophilic/hydrophobic characteristic and chelating capacity, pH, temperature, and reaction time.

Conclusions

Chitosan-PVA composite films are ultraviolet-visible films with good transparency properties as indicated by transmittance percentages above 50 percent at MFC filler loading from 0.5 to 5 percent. The films reinforced with MFC filler loading at 0.5 to 5 percent had slightly better dispersion, miscibility, and uniformity over the film with loading at 7.5 percent. The reinforcement of chitosan-PVA with MFC slightly increased the 2θ diffractograms for amorphous and shoulder peak, whereas the diffractograms of the films' crystalline peaks varied. The films' peaks comprised a crystalline peak 2θ = 11.42° to 11.91°, an amorphous peak at 2θ = 19.66° to 19.83°, and a small ancillary peak at 2θ = 40.62° to –41.03°. The addition of MFC at a filler loading of 0.5 to 5 percent to chitosan-PVA polymer blends shifted FTIR peaks compared to those of neat chitosan-PVA composite film. The addition of MFC notably increased the glass transition temperature of chitosan-PVA nanocomposite films (60.72°C to 67.42°C) but decreased the melting point temperature (124.37°C to 145.59°C). Thermal degradation of chitosan-PVA-MFC nanocomposite film had three transition phases, consisting of water evaporation (40°C to 190°C), structural degradation (210°C to 350°C), and carbonaceous matter degradation (above 350°C). Most of the composite films reinforced with MFC had higher tensile strength than neat chitosan-PVA films. An optimum tensile strength of 77.4 N/mm^2 was found for the film made from chitosan-PVA reinforced with MFC 5 percent. The incorporation of MFC into chitosan-PVA nanocomposite films did not show antibacterial properties against gram-negative *E. coli* or gram-positive *S. aureus*. In addition, these films did have a ZOI or a ZOII against *C. albicans* and *Ganoderma* sp.

Acknowledgments

We thank the Doctoral Programme for Outstanding Undergraduate Students Secretariat due to the financial support of grant number 180/SP2H/LT/DRM/III/2016 Directorate of Higher Education (DIKTI), Ministry of Research, Technology, and Higher Education (Menristekdikti), Republic of Indonesia. We express sincere gratitude to PT Perkebunan Kelapa Sawit Nusantara VIII, Shizuoka

Table 4.—Analysis of antibacterial and antifungal properties of chitosan–polyvinyl alcohol (PVA) nanocomposite films.[a]

	Antibacterial properties				Antifungal properties			
	Escherichia coli		*Staphylococcus aureus*		*Candida albicans*		*Ganoderma* sp.	
Samples	ZOI	ZOII	ZOI	ZOII	ZOI	ZOII	ZOI	ZOII
Chitosan-PVA	No	No	No	No	No	No	No	No
Chitosan-PVA-MFC 2.5%	No	No	No	No	No	No	No	No
Chitosan-PVA-MFC 5%	No	No	No	No	No	No	No	No
Chitosan-PVA-MFC 7.5%	No	No	No	No	No	No	No	No

[a] ZOI = zone of inhibition; ZOII = zone of inhibition index; MFC = microfibrillated cellulose.

University, Indonesian Institute of Sciences, Forest Products Research and Development Centre, Bogor Agricultural University, Bandung Institute of Technology, Gadjah Mada University, Universitas Indonesia, and National Nuclear Energy Agency for the completion of the research.

Literature Cited

Abdolrahimi, M., M. Seifi, and M. H. Ramezanzadeh. 2016. Study the optical properties of PVA/chitosan/MWCNT films as biodegradable packaging with different ratios of acetic acid concentrations and film thicknesses. *Int. J. Adv. Chem. Eng. Biol Sci*. 3(1):88–89.

Abraham, A., P. A. Soloman, and V. O. Rejini. 2016. Preparation of chitosan-polyvinyl alcohol blends and studies on thermal and mechanical properties. *Procedia Technol*. 24:741–748.

Alhosseini, S. N., F. Moztarzadeh, M. Mozafari, S. Asgari, M. Dodel, A. Samadikuchaksaraei, S. Koargozar, and N. Jalali. 2012. Synthesis and characterization of electrospun polyvinyl alcohol nanofibrous scaffolds modified by blending with chitosan for neural tissue engineering. *Int. J. Nanomed*. 7:25–34.

Arora, S., S. Lal, C. Sharma, and K. R. Aneja. 2011. Synthesis, thermal and antimicrobial studies of chitosan/starch/poly(vinyl alcohol) ternary blend films. *Chem. Sin*. 2(5):75–86.

Azizi, S., M. B. Ahmad, M. Z. Hussein, N. A. Ibrahim, and F. Namvar. 2014a. Preparation and properties of poly(vinyl alcohol)/chitosan blend bionanocomposites reinforced with cellulose nanocrystals/ZnO-Ag multifunctional nanosized filler. *Int. J. Nanomed*. 2014(9):1909–1917.

Azizi, S., M. B. Ahmad, N. A. Ibrahim, M. Z. Hussein, and F. Namvar. 2014b. Preparation and properties of poly(vinyl alcohol)/chitosan blend bio-nanocomposites reinforced by cellulose nanocrystals. *Chin. J. Polym. Sci*. 32(12):1620–1627.

Casey, L. S. and L. D. Wilson. 2015. Investigation of chitosan-PVA composite films and their adsorption properties. *J. Geosci. Environ. Prot*. 3:78–84.

Chen, C. H., F. Y. Wang, C. F. Mao, and C. H. Yang. 2007. Studies of chitosan. I. Preparation and characterization of chitosan/poly(vinyl alcohol) blend films. *J. Appl. Polym Sci*. 105:1086–1092.

Ching, Y. C., A. Rahman, K. Y. Ching, N. L. Sukiman, and C. H. Chuah. 2015. Preparation and characterization of polyvinyl alcohol based composite reinforced with nanocellulose and nanosilica. *BioResources* 10(2):3364–3377.

Choo, K., C. Y. Ching, C. H. Chuah, S. Julai, and N. S. Liou. 2016. Preparation and characterization of polyvinyl alcohol-chitosan composite films reinforced with cellulose nanofiber. *Mater*. 2016(9):644–660.

El-Hefian, E. A., M. M. Nasef, and A. H. Yahaya. 2010. The preparation and characterization of chitosan/poly (vinyl alcohol) blended films. *E-J. Chem*. 7(4):1212–1219.

Fathollahipour, S., A. Mehrizi, A. Ghaee, and M. Koosha. 2015. Electrospinning of PVA/chitosan nanocomposite nanofibers containing gelatin nanoparticles as a dual drug delivery system. *J. Biomed. Mater. Res. Part A* 103A:3852–3862.

Frone, A. N., D. M. Panaitescu, D. Donescu, C. I. Spataru, C. Radovici, R. Trusca, and R. Somoghi. 2011. Preparation and characterization of PVA composite with cellulose nanofibers obtained by ultrasonication. *BioResources* 6(1):487–512.

Kanatt, S. R., M. S. Rao, S. P. Chawla, and A. Sharma. 2012. Active chitosanepolyvinyl alcohol films with natural extracts. *Food Hydrocoll*. 29:290–297.

Kermani, A. S. and N. Esfandiary. 2016. Synthesis and characterization of new biodegradable chitosan/polyvinyl alcohol/cellulose nanocomposite. *Adv. Nanopart*. 5:18–26.

Kouchak, M., A. Ameri, B. Naseri, and K. S. Boldaji. 2014. Chitosan and polyvinyl alcohol composite films containing nitrofurazone: Preparation and evaluation. *Iran. J. Basic Med. Sci*. 2014(17):14–20.

Liu, K., X. Lin, L. Chen, L. Huang, S. Cao, and H. Wang. 2013. Preparation of microfibrillated cellulose/chitosan–benzalkonium chloride biocomposite for enhancing antibacterium and strength of sodium alginate films. *J. Agric. Food Chem*. 61(26):6562–6567.

Lu, J., T. Wang, and L. T. Drzal. 2008. Preparation and properties of microfibrillated cellulose polyvinyl alcohol composite materials. *Compos. Part A* 39:738–746.

Nakano, Y., Y. Bin, M. Bando, T. Nakashima, T. Okuno, H. Kurosu, and M. Matsuo. 2007. Structure and mechanical properties of chitosan/poly(vinyl alcohol) blend films. *Macromol. Symp*. 258: 63–81.

Ostadhossein, F., N. Mahmoudi, M. G. Cid, E. Tamjid, F. J. N. Martos, B. S. Cuadrado, J. M. L. Paniza, and A. Simchi. 2015. Development of chitosan/bacterial cellulose composite films containing nanodiamonds as a potential flexible platform for wound dressing. *Mater*. 8:6401–6418.

Panaitescu, D. M., A. N. Frone, M. Ghiurea, and I. Chiulan. 2015. Influence of storage conditions on starch/PVA films containing cellulose nanofibers. *Ind. Crops Prod*. 70(2015):170–177.

Parida, U. K., A. K. Nayak, B. K. Binhani, and P. L. Nayak. 2011. Synthesis and characterization of chitosan-polyvinyl alcohol blended with cloisite 30b for controlled release of the anticancer drug curcumin. *J. Biomater. Nanobiotechnol*. 2:414–425.

Pavaloiu, R. D., A. S. Guzun, M. Stroescu, S. I. Jinga, and T. Dobre. 2014. Composite films of poly(vinyl alcohol)–chitosan–bacterial cellulose for drug controlled release. *Int. J. Biol. Macromol*. 68:117–124.

Pouranvari, S., F. Ebrahimi, G. Javadi, and B. Maddah. 2016. Chemical cross-linking of chitosan/polyvinyl alcohol electrospun nanofibers. *Mater. Technol*. 50(5):663–666.

Santos, C., C. J. Silva, Z. Buttel, R. Guimaraes, S. B. Pereira, P. Tamagnini, and A. Zille. 2014. Preparation and characterization of polysaccharides/PVA blend nanofibrous membranes by electrospinning method. *Carbohydr. Polym*. 99:584–592.

Shankar, S. and J.-R. Rhim. 2016. Preparation of nanocellulose from micro-crystalline cellulose: The effect on the performance and properties of agar-based composite films. *Carbohydr. Polym*. 135:18–26.

Solikhin, A., Y. S. Hadi, M. S. Yusram, and S. Nikmatin. 2016. Novel isolation of empty fruit bunch lignocellulose nanofibers using different vibration milling times-assisted multimechanical stages. *Waste Biomass Valorization* 8(7):2451–2462.

Solikhin, A., Y. S. Hadi, M. S. Yusram, and S. Nikmatin. 2017a. Morphological, chemical, and thermal characteristics of nanofibrillated cellulose isolated using chemo-mechanical methods. *Makara J. Sci*. 21(2):59–68.

Solikhin, A., Y. S. Hadi, M. S. Yusram, and S. Nikmatin. 2017b. Morphological and chemo-thermal changes of oven-heat treated oil palm empty fruit bunch fibers during dry disk milling. *J. Indian Acad. Wood Sci*. 14(1):9–17.

Zhou, Y., S. Fu, L. Zhang, H. Zhan, and M. V. Levit. 2014. Use of carboxylated cellulose nanofibrils-filled magnetic chitosan hydrogel beads as adsorbents for Pb(II). *Carbohydr. Polym*. 101:75–82.

Zhou, Y. M., Y. S. Fu, L. M. Zheng, and H. Y. Zhan. 2012. Effect of nanocellulose isolation techniques on the formation of reinforced poly(vinyl alcohol) nanocomposite films. *eXPRESS Polym. Lett*. 6(10):794–804.